A Novel Enhanced Active Power Control Maximum Power Point Tracking Algorithm for Photovoltaic Grid Tied systems

Rahul Wilson KOTLA[*], Srinivasa Rao YARLAGADDA
Department of Electrical and Electronics Engineering,
Vignan's Foundation for Science Technology and Research, Vadlamudi, Guntur-522213, AP, India
*krw_eeep@vignanuniversity.org

Abstract—**The PV systems connected to the grid will be a very significant renewable energy source in the power systems. Numerous researchers believe that in approaching years major amount of energy on the planet will be produced by Photovoltaic grid tied systems. For this reason, it is crucial to enhance the performance of Photovoltaic grid tied systems, which is facing voltage instabilities, overloading fluctuations during the disturbances. In order to improve the performance, a novel enhanced active power control strategy with incremental conductance maximum power point tracking is proposed in order to obtain the constant power from the photovoltaic grid tied systems. Both single and two-stage Photovoltaic grid tied systems can be effectively controlled by using this algorithm with a proportional integral controller to enhance the performance and flexible to control the operating region near maximum power point. The proposed algorithm mitigates the power losses significantly by generating very few power oscillations of 0.5 kW to 1 kW and an error of about ±0.5 to ±0.9% which is very less oscillation as compared with the conventional perturb & observe-active power control algorithm. The effectiveness of the proposed algorithm is validated by simulation results along with stability analysis and experimental setup considering diverse operating conditions.**

Index Terms—**inverters, maximum power point tracking, power grids, renewable energy sources, solar power generation.**

I. INTRODUCTION

Day by day due to the globalization of metropolises the electricity utilization got increased so that grids were loaded heavily, to overcome this situation the generating capacity should be raised to come across the demand. In view of this renewable energy resources are greatly encouraged to supply this additional demand. Meanwhile, the Photovoltaic is getting to be one of the most utilized sustainable technology, the ability to extract extreme power from Photovoltaic Grid Tied (PVGT) system effectively is done by using MPPT's. As the PVGT systems are non-linear in nature, the Solar Photovoltaic Array (SPVA) current and power in the PVGT system depends on operating voltage of the SPVA. In order to extract maximum power from the SPVA continuous adjustment of SPVA voltage is to be done. In the literature, lot of techniques were developed and analyzed for PVGT systems, out of which conventional MPPT's like Perturb & Observe (P&O) and Incremental conductance (INC) techniques were widely applied for PVGT systems. In fact, INC MPPT algorithm is an enhanced version of P&O as stated in [1-2]. In P&O algorithm SPVA terminal voltage must be incremented or decremented for each perturbation cycle. When the maximum operating point is reached, the P&O algorithm starts oscillating around that point which results in the loss of SPVA output power, particularly for slow varying environments. But for fast varying atmospheric conditions, the P&O algorithm fails and deviates much more from the operating point, this happens due to its instability to match the varying SPVA power for varying environmental conditions. In order to avoid the drawbacks of P&O algorithm mainly power oscillations at MPP are overcome by laid the basis of INC algorithm which was first presented in [3-4]. The INC algorithm always regulates the terminal voltage of the SPVA according to the operating point voltage, which is the failure step of the P&O algorithm for fast varying environs. The INC algorithm is most suitable for any type of SPVA as it is generic algorithm. It works well for wide varying atmospheric conditions and requires no information about the SPVA. But INC algorithm is complex to implement using discrete components and sensors, however it is simple to implement by using advanced digital controllers and has an additional merit of flexible control for different SPVA [5-7]. In Enhanced active power control (EAPC) operation the INC algorithm is used due to that it inherently having the benefits to overcome the main drawback of P&O algorithm.

A PVGT system primarily comprises of PV Arrays, DC to DC converters, MPPT controller tied with grid and loads. The basic modelling and design principles of PV array is taken from [8]. To make a PVGT framework increasingly effective, the active power output should be controlled up to certain power limits is necessary. In recent times there is a lot of innovative algorithms were developed for improving the efficiency of PVGT systems, out of which Active Power Control (APC) technique also known as constant power generation (CPG) is one of them [9]. There are certain conditions for the adaptation of new PVGT systems where constant power injection to the grid is necessary in order to meet the new grid codes and regulations [10]. The new grid codes are principally focusing to avoid the adverse conditions like high penetration of new PVGTs into the power system, loading the power grid greater than the installed capacities. The new grid codes also state that the voltage at the point of common coupling is to be boosted by injection of active and reactive power to the grid

simultaneously at the time of voltage sags on the grid. During the voltage sags the irradiance is assumed to be constant as the sag appears for a short duration, in order to satisfy the current limitations of the inverter the power extracted from the SPVA should be limited to the certain power reference is needed [11]. By considering the new grid codes and regulations for all the topologies of PVGT systems a common algorithm is essential that should control the active power of the system with low power oscillations and fast dynamic response. The main topologies of PVGT systems are shown in Fig.1 and Fig. 2.
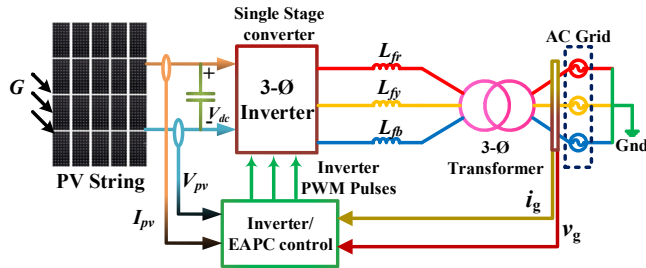

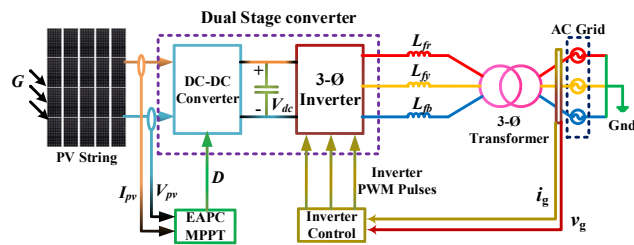Figure 1. Single-Stage PVGT System

Figure 2. Dual-Stage PVGT System

The basic design concepts of APC strategy were presented in [12] and [13-17], which gives the DC-DC converter and inverter control concepts to achieve the maximum power from the PVGT systems. But the basic theme of these concepts was only discussed about the stability concerns of the inverter real power outputs for single-stage PVGT systems. The APC along with P&O technique were designed based on the voltage constraint is discussed in [9], [15] to control the real power. But due to the single-stage topology when there is a rapid change in Irradiance (G) the MPP will shift aside of the V_{mpp} and may cross the V_{oc} point, this will decrease the reliability of PVGT system [16], [18]. For this reason, advanced dual-stage PVGT systems were discussed in [19] to attain dual mode of operation of APC along with MPPT which will shifts the operating point besides the V_{mpp} point in order to avoid the output voltage crossing the V_{oc} point. But these systems have to change its mode of operation based on the output power will result in a poor response of the system.

For this reason, a common concept was designed to overcome the demerits of both the systems discussed above in [20], this algorithm is applicable to both the single and dual-stage PVGT systems along with APC and P&O algorithms. But as compared with the existing APC strategy with conventional P&O MPPT technique, the major advantage in this proposed APC strategy is that when it operates in MPPT mode with INC technique, its output voltage, and output power oscillations during MPPT mode were reduced and the tracking efficiency is increased. The other thing is that it can also be able to shift the MPP to Right or Left side of MPP for both single and dual stage

PVGT systems.

In the literature of PVGT systems with CPG or APC only discussed P&O MPPT algorithm as a part of APC either for single or for the dual stage [21], [23]. In this paper a novel EAPC strategy is proposed for PVGT systems, in which INC MPPT algorithm is coordinated along with the APC called an EAPC strategy is discussed for both single and dual stage systems to overcome the drawbacks of APC with conventional P&O MPPT. The rest of the Paper organizes as follows: section II presents the basic methodology of APC for PVGT systems, section III presents the proposed EAPC algorithm, section IV stability analysis of proposed system, section V presents the simulation results for proposed strategy, section VI presents the experimental verifications and section VII concludes the paper.

II. BASIC METHODOLOGY OF APC

In this section, the basic theory of APC was discussed which was discussed in [9] and [22]. The main aim of APC is to design the PVGT systems more economically by controlling the MPPT at the Inverter stage or at the charge controller stage commonly known as DC-DC converter stage. Basically, this strategy operates in two modes i.e., MPPT mode and APC mode. Based on the available power from the PV two operating modes were presented as presented in Fig. 3.
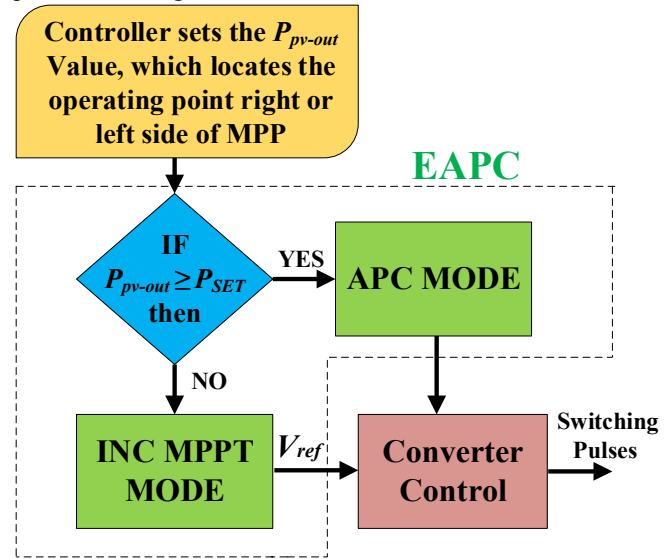

Figure 3. Control Structure of single and dual stage PVGT systems

MPPT mode: In this mode, MPPT with INC technique is proposed rather than P&O for enhanced tracking efficiency with reduced oscillations in the output power during this mode of operation. For the MPPT mode of operation, the power generated from the PV string (P_{pvs}) is less than the set value of power (P_{set}). So, the instantaneous power output (P_{out-pv}) will be given as.

$$P_{pv-out} = P_{INC-MPPT} \qquad (1)$$

When $P_{pvs} < P_{set}$ the controllers work at INC MPPT mode.

APC Mode: In this mode, the P_{PVS} is set to a reference power which is normally less than the power output of PV. For APC mode the power generated from PV string $P_{pvs} = P_{set}$. This strategy uses a PI controller which has fast dynamic performance and reduced power oscillations during steady-state and transient conditions.

The PVS operates in two regions x and y around its MPP as presented in Fig. 4. The magnitude of both x and y are the same and set to P_{set} value indicated by the blue dotted line in Fig. 4. As the magnitude of both x and y are the same but it lies in the left and right side of MPP. The left and right side operation around MPP has its own merits and demerits [23].
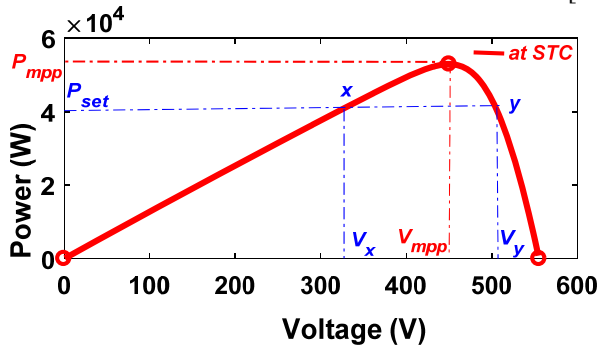

Figure 4. Operating points x and y of P-V plot for P_{set} value

A. Operating Point at x

By choosing the operating point at x the system response will be as follows:

- In PVGT systems the output voltage of PVS should be approximately close to short circuit voltage (V_{sc}) in order to obtain the high efficiency operation of the system. At x the voltage (V_x) is very less as compared to the V_{sc}, so that the duty cycle (D) of the charge controller should be increased to unity. If D is increased approximately to unity, then there may be huge disturbances at the charge controller input and output voltage as well as in currents.
- The voltage variance between V_x and V_{mpp} is considerably large and has more power oscillation in output power of PVS and inductor gets distorted.

B. Operating Point at y

By choosing the operating point at y the system response will be as follows:

- In PVGT systems the voltage of PVS at point y is V_y, and the variance of this voltage from V_{mpp} is small. Hence the system response is fast as compared to the response at point x. But if there is a slight alteration in the G and T will generate huge oscillations in the PVS output power as compared with the oscillations at x.
- The point y lies on the right side of MPP, which will lead the system voltage over the open-circuit voltage (V_{oc}) when there is a fast alteration of the PV inputs. This the main design consideration while developing the EAPC algorithm.

III. ENHANCED ACTIVE POWER CONTROL ALGORITHM

The P&O APC algorithm works well only for slow varying irradiance, but for fast varying irradiance, this conventional method generates huge power oscillations as discussed in [2]. To overcome this a high performance P&O APC strategy was discussed in [20]. But this paper uses the APC strategy along with INC to reduce the power oscillations considerably as compared to P&O. The EAPC of PVS can be developed by observing the P-V characterizes operating at x or y points. The instantaneous values of voltage (ΔV) are the difference between the present voltage

$V_{present}$ and previous voltage $V_{previous}$. Likewise for instantaneous power (ΔP) is the difference between the present power $P_{present}$ and previous power $P_{previous}$.

$$\Delta V = V_{present} - V_{previous} \qquad (2)$$

$$\Delta P = P_{present} - P_{previous} \qquad (3)$$

For MPPT mode the voltage execution time ($T_{ex-mppt}$) and the voltage execution between different operating points ($V_{ex-mppt}$) are taken quite a lager and smaller respectively, in order to reduce the power oscillations in the P_{pv-out}. The basic principles of $T_{ex-mppt}$ and $V_{ex-mppt}$ were discussed clearly in [9]. The complete operational flowchart of the EAPC strategy is presented in Fig. 6.

Based on the conditions stated in (1) and (2) the EAPC strategy selects its mode of operation. In the APC mode, the hysteresis controller is used in order to work the PVGT systems well in both Fault and Healthy conditions. The hysteresis controller is used to decide the value of real power when there is a fault in the system, under healthy conditions it is used to stabilize the system quickly by reducing the power oscillations. In order to achieve this by hysteresis controller in Faulty and healthy situations, various values of Voltages (V_{APC}) and Time periods (T_{APC}) are to be considered.

If there is a Fault in the system APC strategy directly sets the controller to the execution voltage of APC at Fault ($V_{ex-APC-Fault}$) and a Time ($T_{ex-APC-Fault}$). If the system is healthy then it will check for $|\Delta P| > \Delta P_{hold}$, where ΔP_{hold} is threshold power sets to 8 kW in this algorithm. If $|\Delta P| > \Delta P_{hold}$ is true then it senses that there is a transient or fault in the system so that it sets to V_{APC} and T_{APC} to $V_{ex-APC-Fault}$ and $T_{ex-APC-Fault}$ respectively. If the condition $|\Delta P| > \Delta P_{hold}$ is false then it checks for $\Delta P / \Delta P_{previous} > 0$, if it is true then it again sets V_{APC} and T_{APC} to the Fault conditions. If the condition $\Delta P / \Delta P_{previous} > 0$ is false then it sets the V_{APC} and T_{APC} to the normal execution voltage of APC ($V_{ex-APC-normal}$) and time ($T_{ex-APC-normal}$) of APC. For the operating points of x and y the APC algorithm checks for the conditions of $\Delta P / \Delta V > 0$ and $\Delta P / \Delta V < 0$. Based on these above conditions the set voltage (V_{set}) is fixed for the APC mode and decides the operating regions about MPP.
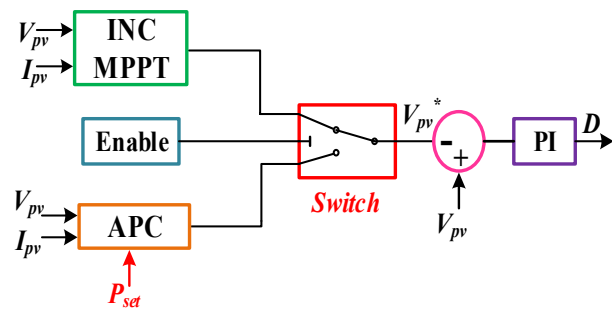

Figure 5. EAPC strategy with PI controller

The key concept in this paper is the introduction of INC MPPT algorithm along with the APC. In this MPPT mode, this strategy uses conventional Incremental conductance (INC) algorithm as shown in Fig. 6. This algorithm is used due to the main reason that it reduces the power oscillations drastically as compared to the conventional P&O. The EAPC strategy along with the PI controller is shown in Fig. 5. The output of EAPC strategy is fed through a PI

controller which enhance the dynamic response of the system and also generates the switching pulses for DC-DC converter and Inverter switches for dual stage systems and single stage systems respectively.
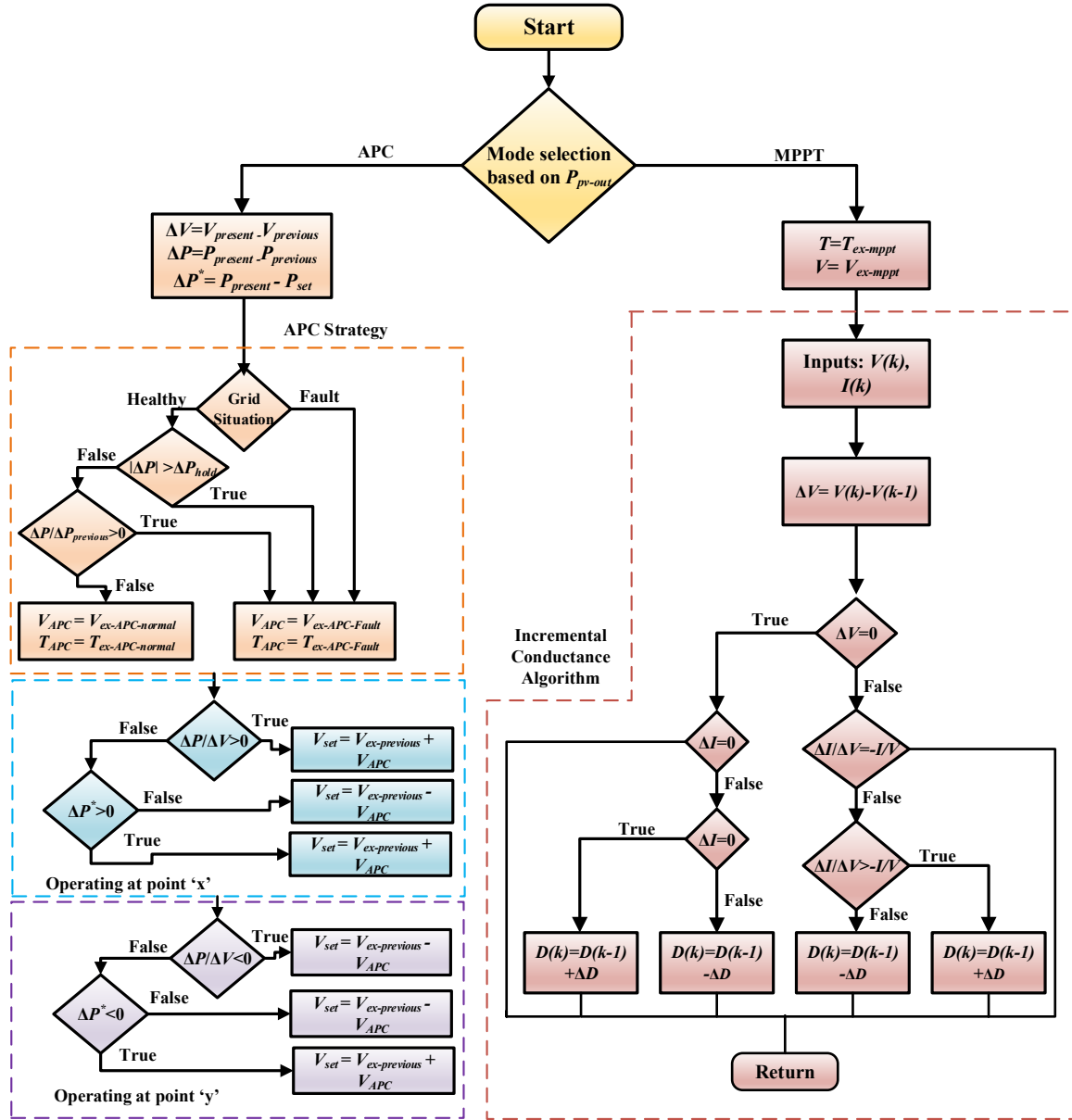

Figure 6. Operational Flowchart of EAPC strategy

IV. STABILITY ANALYSIS OF PROPOSED SYSTEM

The proposed EAPC algorithm is realized by using a boost converter. The PV panel connected to the Boost Converter is shown in Fig.7.
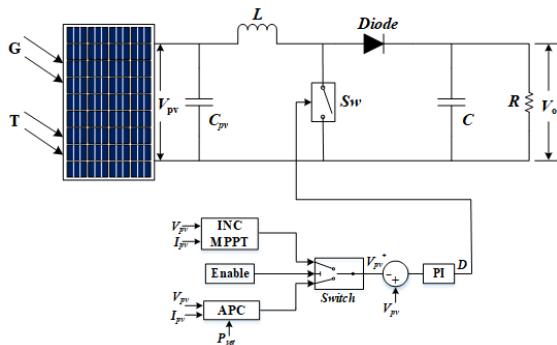

Figure 7. Operational Flowchart of EAPC strategy

According to the averaging method of state space model used in [24]-[26], the transfer function of proportional integral (PI) controller is given by

$$G_c(s) = K_p + \frac{K_i}{s} \qquad (4)$$

The open loop transfer function (OLTF) of the proposed system is given by

$$G_{OL}(s) = G_d(s)G_c(s) \qquad (5)$$

where,

$$G_d(s) = \frac{V_o C s + 2\frac{V_o}{R}}{LCs^2 + \frac{L}{R}s + (1-D)^2} \qquad (6)$$

The boost converter nominal switching frequency is considered as 20 kHz. The PI controller parameters $K_p = 0.252$ and $K_i = 0.63$ is calculated from Bode diagram by using phase and Gain margins. For the proposed system, the PI controller is designed for 50 kW system on simulation platform and 1 kW system on experimental platforms and found that the system is stable from the Bode diagram of OLTF.
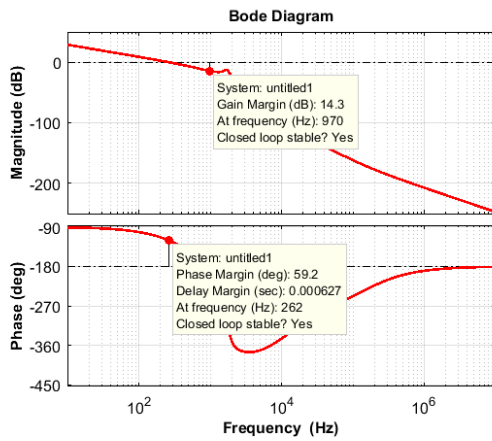
Figure 8. Stability analysis using Bode diagram

V. SIMULATION RESULTS

The single stage and dual stage PVGT systems were designed using the Matlab/Simulink environment. The parameters used in this system is shown in Table 1. The input irradiance profile for this investigation for the conventional and proposed system is presented in Fig. 9, which is taken from the conventional method [9] and the input profile is updated with the additional values of G by considering the worst value of G i.e., 0.4 kW/m^2 and a peak value of 1.25 kW/m^2. The proposed input profile considers wide values of G like over and under the STC are considered in order to validate the performance of the proposed algorithm. By using the proposed algorithm both single and dual stage PVGT systems output profiles were obtained. A total of 6 modes of operation were considered in order to simulate and compare the proposed algorithm with the conventional method.
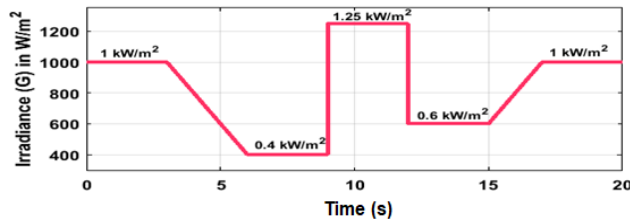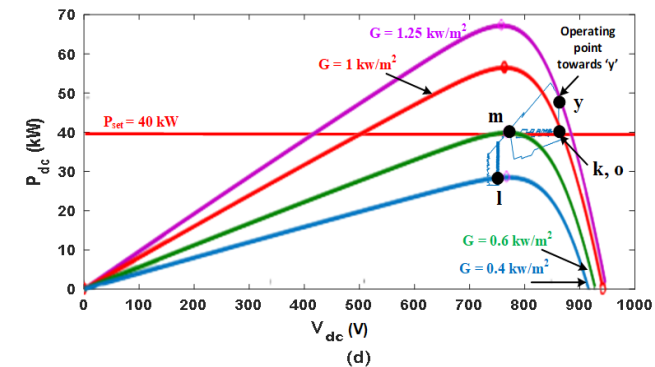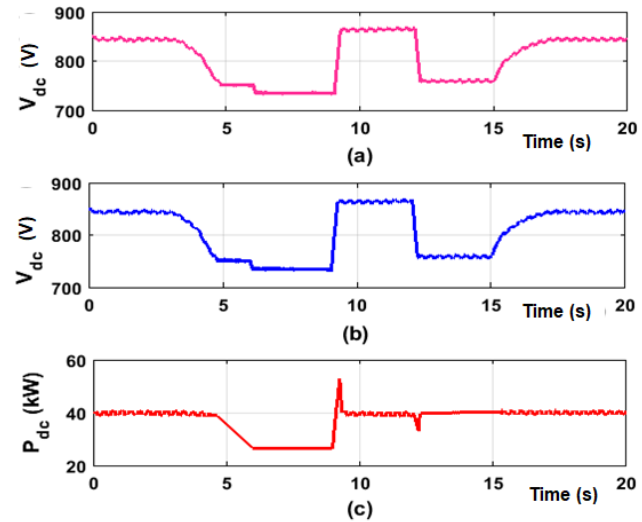

Figure 9. Input Irradiance profile (W/m^2)

TABLE I. PVGT SYSTEM SIMULATION PARAMETERS

Parameters	Single stage system	Two stage systems
Total PVGT system power (P_{system})	50000 W	50000 W
Peak panel power (P_{mpp})	235 W	235 W
Current at peak power (I_{mpp})	7.84 A	7.84 A
Voltage at peak power (V_{mpp})	30 V	30 V
Fill Factor	0.72	0.72
Grid Bus voltage (V_g) in rms	430 V	430 V
Voltage at DC bus (V_{dc})	770 V	770 V
Capacitor at DC-link	5*10^{-3} F	5*10^{-3} F
Series tied modules in the string	25	15
Parallel tied modules in the string	9	15
Input Inductance of Boost	10*10^{-3} H	10*10^{-3} H

converter		
Boost converter capacitor	12*10^{-3} F	12*10^{-3} F
Set power of APC (P_{set})	40 kW	40 kW
Execution time of INC MPPT ($T_{ex-mppt}$)	0.1 s	0.1 s
Execution voltage of INC MPPT ($V_{ex-mppt}$)	5 V	5 V
Execution time of APC at normal conditions ($T_{ex-APC-normal}$)	0.1 s	0.1 s
Execution time of APC at fault ($T_{ex-APC-fault}$)	0.002 s	0.002 s
Execution voltage of APC at normal ($V_{ex-APC-normal}$)	At 'y' is 1 V At 'x' is 6 V	At 'y' is 1 V At 'x' is 6 V
Execution voltage of APC at fault ($V_{ex-APC-fault}$)	At 'y' is 3 V At 'x' is 8 V	At 'y' is 3 V At 'x' is 8 V
Threshold Power (ΔP_{hold})	8 kW	8 kW

Mode I. The conventional APC algorithm without any MPPT, means APC alone [9] for single stage PVGT system is presented in Fig. 10. In this mode the operating point shifts towards the point 'y' i.e., the right side of the PV curve as shown in Fig. 10(d).

Figure 10. Conventional CPG algorithm for single stage system: (a) DC reference voltage (b) PV output voltage (V_{dc}), (c) PV output power (P_{dc}) and (d) PV- plot showing the operating point shifts towards 'y'

At t = 3 s, the G is 1 kW/m^2 and the voltage sets to 850 V which sets the operating point at point 'k' as shown in Fig. 10(d). The voltage and time execution of APC is taken as 6 V and 0.1 s respectively, which will generate the power oscillation until t = 4 s. At this instant, the set power (P_{set}) is greater the generated power from the PV string, where the

P_{set} for APC mode is considered as 40 kW. During $t = 6$ to 9 s, the operating point is at 'l' and is at G of 0.4 kW/m², which is exactly at the MPP of that curve. At time $t = 9$ s the value of G increases drastically beyond the STC and sets to 1.25 kW/m² and the operating point shifts towards the point 'y'. Finally, if G decreases to 0.6 kW/m² at $t = 12$ s the operating point is at point 'm', at this instant the P_{dc} is approximately equaled to the P_{set}. Further, if the G increases again to STC then the operating point shifts to the point 'o' which is same as the point 'k'. This mode generates a power oscillation of 1 to 2 kW and an error of about ±1 to ±2% and the complete operation states the operating point reaches around the right of MPP. The dc voltage reference (V_{dc-ref}) at APC, PV output voltage (V_{dc}) at the inverter input and PV output power (P_{dc}) is presented in Fig. 10(a), Fig. 10(b), and Fig. 10(c) respectively.

Mode II. The conventional APC algorithm alone without any MPPT [9] for dual stage PVGT system is presented in Fig. 11. In this mode, the operating point shifts towards the point 'x' i.e., left the side of the PV curve as shown in Fig. 11(d).
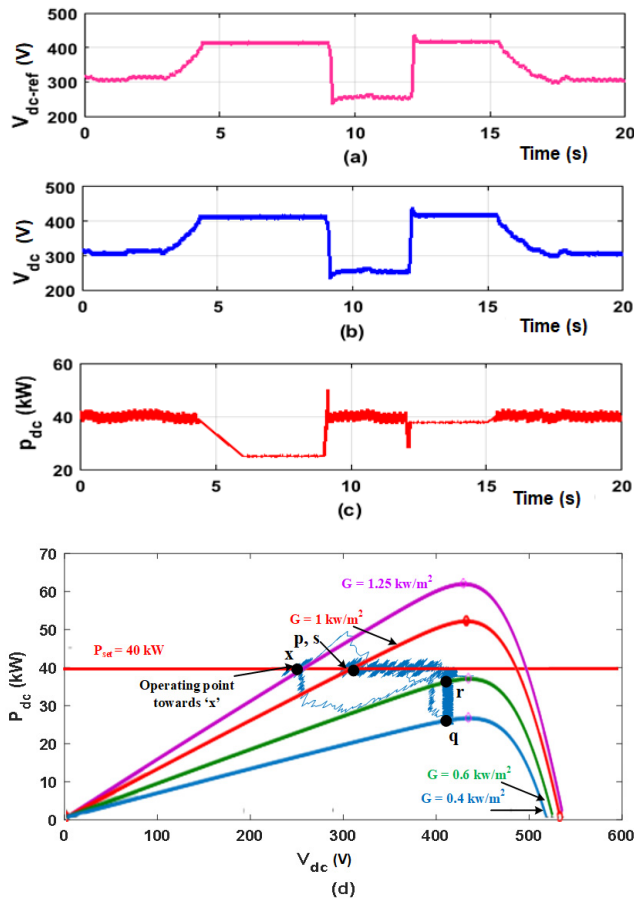
the MPP of that curve. At time $t = 9$ s the value of G increases drastically beyond the STC and sets to 1.25 kW/m² and the operating point shifts towards the point 'x'. Finally, if G decreases to 0.6 kW/m² at $t = 12$ s the operating point is at point 'r', at this instant the P_{dc} is approximately equaled to the P_{set}. Further, if the G increases again to STC then the operating point shifts to the point 's' which is same as the point 'p'. This mode also generates power oscillations of 1 kW to 2 kW and an error of about ±1 to ±2% for dual stage systems. The dc voltage reference (V_{dc-ref}) at APC, PV output voltage (V_{dc}) at the inverter input and PV output power (P_{dc}) is shown in Fig. 11(a), Fig. 11(b), and Fig. 11(c) respectively.

Mode III. The conventional APC algorithm alone without any MPPT [9] for dual stage PVGT system is presented in Fig. 12, with the operating point shifts towards the point 'y' i.e., the right side of the PV curve as presented in Fig. 12(d). At $t = 3$ s, the G is 1 kW/m² and the voltage sets to 310 V which sets the operating point at point 'k' as shown in Fig. 12 (d).
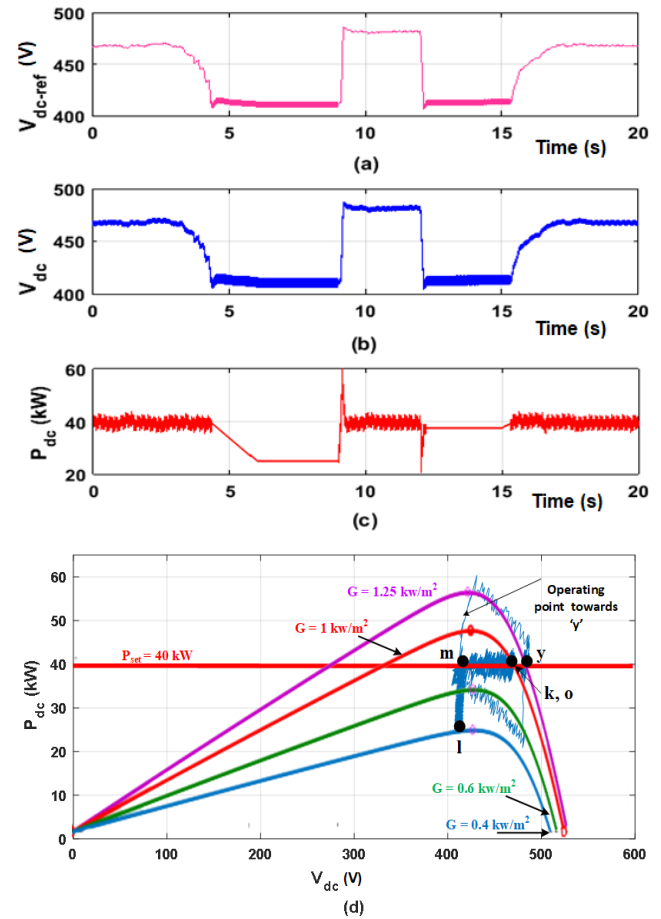

Figure 11. Conventional CPG algorithm for Dual stage system: (a) DC reference voltage (b) PV output voltage (V_{dc}), (c) PV output power (P_{dc}) and (d) PV- plot showing the operating point shifts towards 'x'

Figure 12. Conventional CPG algorithm for Dual stage system: (a) DC reference voltage (b) PV output voltage (V_{dc}), (c) PV output power (P_{dc}) and (d) PV- plot showing the operating point shifts towards 'y'

At $t = 3$ s, the G is 1 kW/m² and the voltage sets to 310 V which sets the operating point at point 'p' as shown in Fig. 11(d). The $V_{ex-APC-normal}$ and $T_{ex-APC-normal}$ are taken as 1 V and 0.1 s respectively for healthy condition and for Fault or transient conditions the $V_{ex-APC-fault}$ and $T_{ex-APC-fault}$ is 3 V and 0.002 s respectively, which will generate the power oscillation until $t = 4$ s. During $t = 6$ to 9 s, the operating point is at 'q' and is at G of 0.4 kW/m², which is exactly at

The $V_{ex-APC-normal}$ and $T_{ex-APC-normal}$ are taken as 1 V and 0.1 s respectively for healthy condition and for Fault or transient conditions the $V_{ex-APC-fault}$ and $T_{ex-APC-fault}$ is 3 V and 0.002 s respectively, which will generate the power oscillation until $t = 4$ s. During $t = 6$ to 9 s, the operating point is at 'l' and is at G of 0.4 kW/m², which is exactly at the MPP of that curve. At time $t = 9$ s the value of G increases drastically beyond the STC and sets to 1.25 kW/m² and the operating point shifts towards the point 'y'. Finally, if G decreases to

0.6 kW/m² at t = 12 s the operating point is at point 'm', at this instant the P_{dc} is approximately equaled to the P_{set}. Further, if the G increases again to STC then the operating point shifts to the point 'o' which is same as the point 'k'. This mode also generates power oscillations of 1 kW to 2 kW and an error of about ±1 to ±2% for dual stage systems. The dc voltage reference (V_{dc-ref}) at APC, PV output voltage (V_{dc}) at the inverter input and PV output power (P_{dc}) is shown in Fig. 12(a), Fig. 12(b), and Fig. 12(c) respectively.

Mode IV. The proposed APC algorithm with INC MPPT called an EAPC strategy for single stage PVGT system is presented in Fig. 13, with the operating point shifts towards the point 'y' i.e., left the side of the PV curve as shown in Fig. 13(e). The proposed algorithm able to shift the INC MPPT mode to APC by taking the two set powers P_{set1} and P_{set2} as 35 kW and 25 kW, respectively. At t = 0 to 3 s, the voltage gets increased to 881 V as shown in Fig.13(a), which sets the operating point at point 'y' for the set power of P_{set1} = 35kW as shown in Fig. 13(e). The $V_{ex-APC-normal}$ and $T_{ex-APC-normal}$ are taken as 6 V and 0.1 s respectively for healthy condition and for fault or transient conditions the $V_{ex-APC-fault}$ and $T_{ex-APC-fault}$ is 8 V and 0.002 s, respectively. During t = 6 to 9 s, the operating point is at 'k', for the set power of P_{set2}=25kW. At this instant, the voltage may go beyond the open-circuit voltage. At time t = 9 s, the value of G decreases drastically to 0.3 kW/m² and the operating point shifts towards the point 'l', which is exactly at the MPP of that curve. This proposed mode generates very fewer power oscillations of 0.5 kW to 1 kW and an error of about ±0.5 to ±0.9% which is very less oscillation as compared with conventional P&O algorithm for single stage systems as noticed from Fig. 13. The conventional and proposed PV output voltage (V_{dc}) at the inverter input and PV output power (P_{dc}) is shown in Fig 13(a), 13(b), 13(c), and 13(d) respectively.
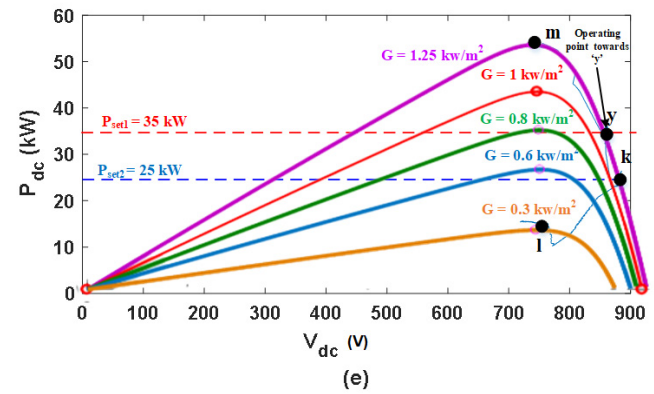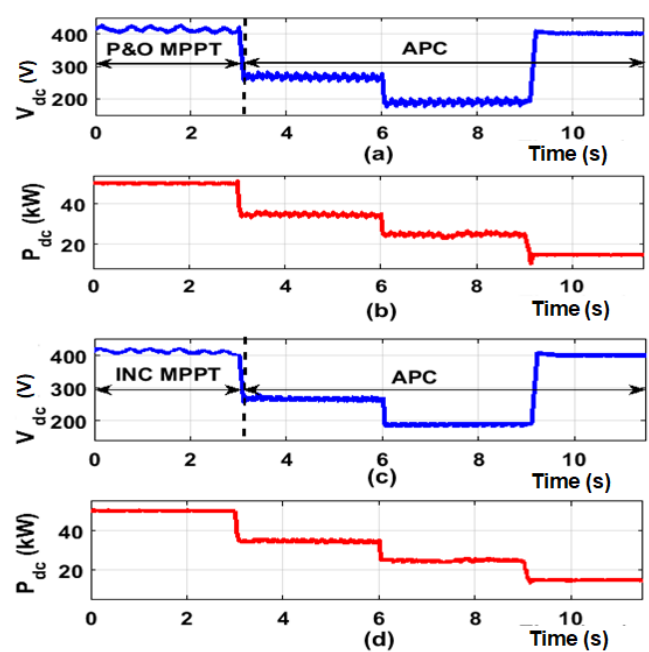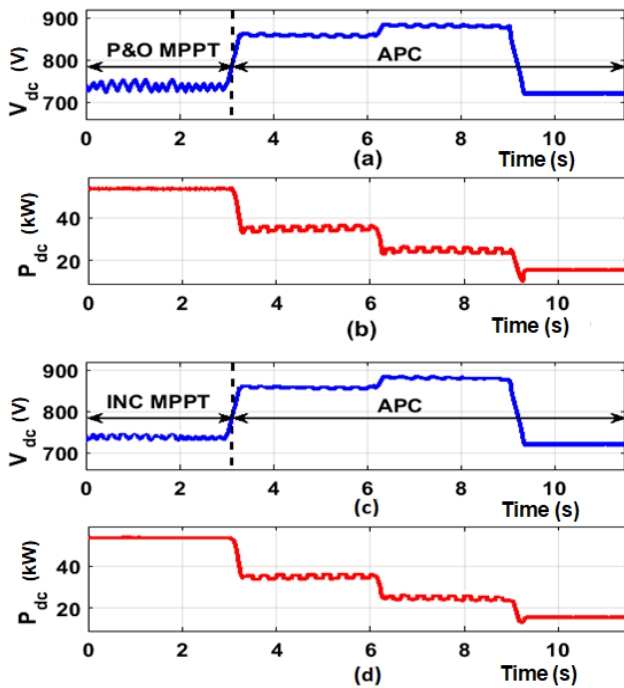

Figure 13. Proposed EAPC strategy for single stage PVGT system. (a) PV output voltage (V_{dc}) of Conventional APC with P&O MPPT, (b) PV output power (P_{dc}) of Conventional APC with P&O MPPT (c) PV output voltage (V_{dc}) of proposed EAPC strategy, (d) PV output power (P_{dc}) of proposed EAPC strategy (e) PV- plot showing the operating point shifts towards 'y'

Mode V. The proposed APC algorithm with INC MPPT called an EAPC strategy for dual stage PVGT system is presented in Fig. 14, with the operating point shifts towards the point 'x' i.e., left the side of the PV curve as shown in Fig. 14(e). The proposed algorithm able to shift the INC MPPT mode to APC by taking the two set powers P_{set1} and P_{set2} as 35 kW and 25 kW, respectively. At t = 0 to 3 s, the voltage gets increased to 410 V as shown in Fig.14(a), which sets the operating point at point 'y' for the set power of P_{set1} = 35kW as shown in Fig. 14(e). The $V_{ex-APC-normal}$ and $T_{ex-APC-normal}$ are taken as 1 V and 0.1 s respectively for healthy condition and for fault or transient conditions the $V_{ex-APC-fault}$ and $T_{ex-APC-fault}$ is 3 V and 0.002 s, respectively. During t = 6 to 9 s, the operating point is at 'p', for the set power of P_{set2}=25kW. At time t = 9 s, the value of G decreases drastically to 0.3 kW/m² and the operating point shifts towards the point 'q', which is exactly at the MPP of that curve.
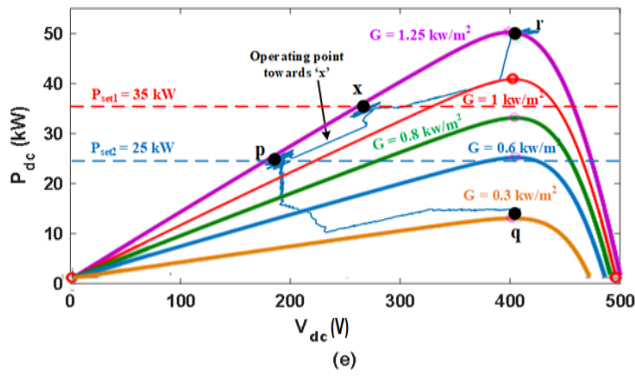
Figure 14. Proposed EAPC strategy for dual stage PVGT system. (a) PV output voltage (V_{dc}) of Conventional APC with P&O MPPT, (b) PV output power (P_{dc}) of Conventional APC with P&O MPPT (c) PV output voltage (V_{dc}) of proposed EAPC strategy, (d) PV output power (P_{dc}) of proposed EAPC strategy (e) PV- plot showing the operating point shifts towards 'x'

This proposed mode generates very fewer power oscillations of 0.5 kW to 1kW and an error of about ±0.5 to ±0.9% which is very less oscillation as compared with conventional P&O algorithm for dual stage systems as noticed from Fig. 14. The conventional and proposed PV output voltage (V_{dc}) at the inverter input and PV output power (P_{dc}) is shown in Fig 14(a), 14(b), 14(c), and 14(d) respectively.

Mode VI: The proposed APC algorithm with INC MPPT called an EAPC strategy for dual stage PVGT system is presented in Fig. 15, with the operating point shifts towards the point 'y' i.e., left the side of the PV curve as shown in Fig. 15(e). The proposed algorithm able to shift the INC MPPT mode to APC by taking the two set powers P_{set1} and P_{set2} as 35 kW and 25 kW respectively. At $t = 0$ to 3 s, the voltage gets increased to 430 V as shown in Fig.15 (a), which sets the operating point at point 'y' for the set power of $P_{set1} = 35$kW as shown in Fig. 15(e). The $V_{ex-APC-normal}$ and $T_{ex-APC-normal}$ are taken as 6 V and 0.1 s respectively for healthy condition and for Fault or transient conditions the $V_{ex-APC-fault}$ and $T_{ex-APC-fault}$ is 8 V and 0.002 s respectively. During $t = 6$ to 9 s, the operating point is at 'k', for the set power of P_{set2}=25kW. At this instant, the voltage may go beyond the open-circuit voltage. At time $t = 9$ s, the value of G decreases drastically to 0.3 kW/m² and the operating point shifts towards the point 'l', which is exactly at the MPP of that curve.
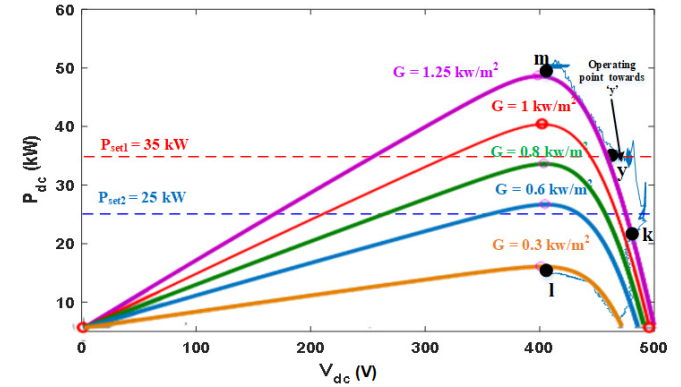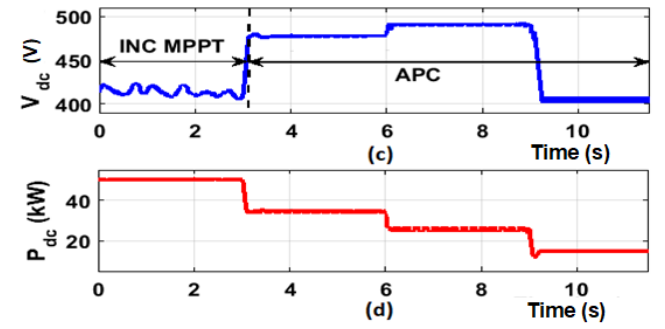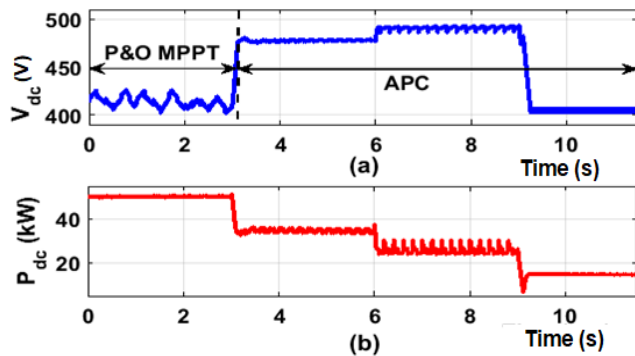

Figure 15. Proposed EAPC strategy for dual stage PVGT system. (a) PV output voltage (V_{dc}) of Conventional APC with P&O MPPT, (b) PV output power (P_{dc}) of Conventional APC with P&O MPPT (c) PV output voltage (V_{dc}) of proposed EAPC strategy, (d) PV output power (P_{dc}) of proposed EAPC strategy (e) PV- plot showing the operating point shifts towards 'y'

This proposed mode generates very fewer power oscillations of 0.5 kW to 1 kW and an error of about ±0.5 to ±0.9% which is very less oscillation as compared with conventional P&O algorithm for single stage systems as noticed from Fig. 15. The conventional and proposed PV output voltage (V_{dc}) at the inverter input and PV output power (P_{dc}) is shown in Fig 15(a), 15(b), 15(c), and 15(d) respectively.

Finally, the proposed EAPC strategy results in better performance by reducing the voltage and power oscillations sensitively in the output as compared with the conventional APC strategy with P&O which is available in the literature. The proposed EAPC strategy is robust and able to operates at both sides of MPP within the safety limits along with the improved performance by reducing the output power oscillations.

VI. EXPERIMENTAL VERIFICATION

The proposed novel EAPC strategy is implemented by using a 1 kW PVGT system along with a DC-DC converter, INC MPPT controller and the Inverter circuits. The INC MPPT controller is realized using the 1708066 μC Microchip, the boost converter and Inverter switches are realized using silicon IRPF 150N MOSFET devices are shown in Fig. 16 and Fig. 17. The experimental results present the output powers for both APC along with P&O and APC with INC strategy. Two operating modes were considered in order to obtain the performance of both systems.
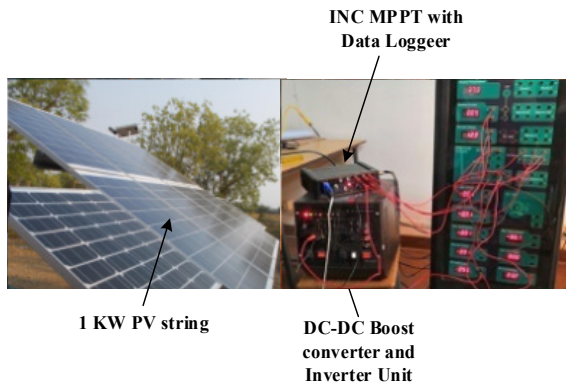
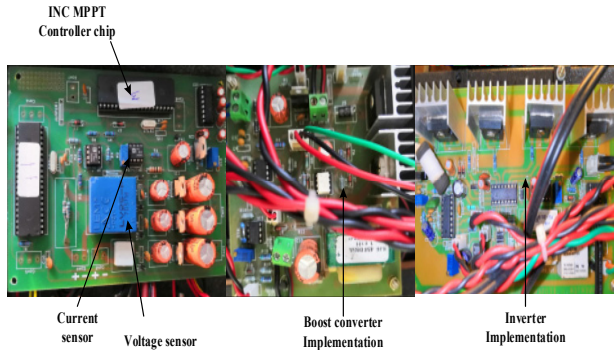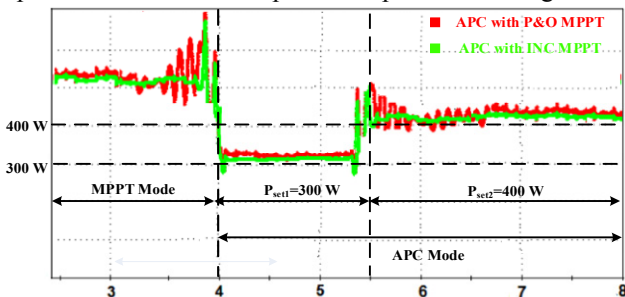Figure 16. Overall Experimental setup for EAPC strategy

Figure 17. Experimental setups for MPPT, DC-DC Boost converter and Inverter

Mode I: The converter operates in MPPT mode up to $t = 4$ s, and at $t = 4$ s to 5.5 s the controller sets the power to $P_{set1} = 300$ W. It is noticed that during this transition from one mode to another mode APC with P&O generates high power oscillations as compared with the APC with INC as presented in Fig. 18. At $t = 5.5$ s the controller sets the power to $P_{set2} = 400$W, then the output power gets shifted P_{set1} to P_{set2}. As compared with the conventional APC with P&O, it is clear that from the results obtained the proposed algorithm has fewer power oscillations during MPPT mode, APC mode as well as the transition periods also. By taking the values from experimental setup using data logger the experimental results were plotted as presented in Fig. 18.

Figure 18. Experimental results of EAPC strategy for P_{set1} and P_{set2}

Mode II: The converter operates in MPPT mode during $t = 0$ to 4 s and from $t = 5.5$ s. This mode linearly decreases values of G from STC to 300 W/m^2 and the output powers in both cases were plotted as presented in Fig.19. At $t = 4$ s to 5.5 s, the controller sets the power P_{set1} to 300 W along with the decrease in the G to 700 W/m^2. It is noticed that during this transition from one mode to another mode APC with P&O generates high power oscillations as compared with the APC with INC. At $t = 5.5$ s the controller again operates in MPPT mode, then the output power gets

decreases to around 200 W. As compared with the conventional APC with P&O, it is clear that from the results obtained the proposed algorithm has fewer power oscillations during MPPT mode, APC mode as well as the transition periods also. In this mode also APC with INC MPPT has better results as compared with the conventional method.
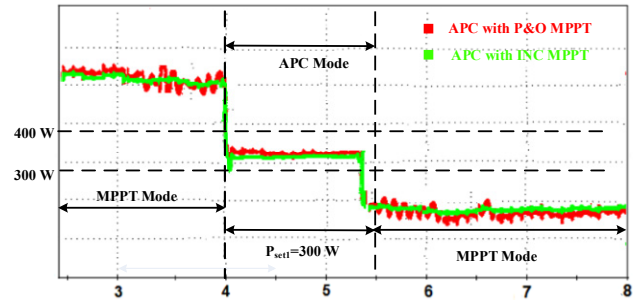

Figure 19. Experimental results of EAPC strategy for linear decrease of irradiance

VII. CONCLUSION

The proposed novel enhanced active power control strategy will enhance the tracking efficiency significantly and reduces the power oscillations during maximum power point tracking mode as compared to the previous active power control with perturb & observe existed in the literature. The proposed algorithm mitigates the power losses significantly by generating very few power oscillations of 0.5 kW to 1 kW and an error of about ±0.5 to ±0.9 % which is very less oscillation as compared with the conventional perturb & observe -active power control algorithm which generates a power oscillation of 1 kW to 2 kW and an error of about ±1 to ±2 %. This algorithm also moves the operating point to the right or left-side of maximum power point region and flexible to operate for single- or two-stage photovoltaic grid tied systems. During steady state and varying irradiance conditions the active power control algorithm along with incremental conductance maximum power point tracking will results in reduced power oscillations and the proportional integral controller is used for obtaining quick dynamic response. The simulation and experimental validations reveal its generality and applicability to the photovoltaic grid tied systems with reduced power oscillations.

REFERENCES

[1] S. Xu, Y. Gao, G. Zhou and G. Mao, "A Global Maximum Power Point Tracking Algorithm for Photovoltaic Systems Under Partially Shaded Conditions Using Modified Maximum Power Trapezium Method," in IEEE Transactions on Industrial Electronics, vol. 68, no. 1, pp. 370-380, Jan. 2021. doi:10.1109/TIE.2020.2965498

[2] F. A. Silva, "Power electronics and control techniques for maximum energy harvesting in photovoltaic systems," (Femia, N. et al; 2013) [Book News], in IEEE Industrial Electronics Magazine, vol. 7, no. 3, pp. 66-67, Sept. 2013. doi:10.1109/MIE.2013.2272239

[3] Y. Zhu, H. Wen, G. Chu, Y. Hu, X. Li and J. Ma, "High-performance photovoltaic constant power generation control with rapid maximum power point estimation," in IEEE Transactions on Industry Applications, vol. 57, no. 1, pp. 714-729, Jan.-Feb. 2021. doi:10.1109/TIA.2020.3029128

[4] K. R. Wilson and Y. S. Rao, "Comparative analysis of MPPT algorithms for PV grid tied systems: A Review," 2019 2nd International Conference on Intelligent Computing, Instrumentation and Control Technologies (ICICICT), 2019, pp. 1105-1110. doi:10.1109/ICICICT46008.2019.8993148

[5] R. Bakhshi-Jafarabadi, J. Sadeh and M. Popov, "Maximum power point tracking injection method for islanding detection of grid-connected photovoltaic systems in microgrid," in IEEE Transactions on Power Delivery, vol. 36, no. 1, pp. 168-179, Feb. 2021. doi:10.1109/TPWRD.2020.2976739

[6] R. W. Kotla and S. R. Yarlagadda, "Power management of PV-battery-based low voltage microgrid under dynamic loading conditions," Journal of The Institution of Engineers (India): Series B, vol. 102, no. 4, pp. 797-806, 2021. doi:10.1007/s40031-021-00544-2

[7] X. Li, H. Wen, Y. Hu, Y. Du and Y. Yang, "A comparative study on photovoltaic MPPT algorithms under EN50530 dynamic test procedure," in IEEE Transactions on Power Electronics, vol. 36, no. 4, pp. 4153-4168, April 2021. doi:10.1109/TPEL.2020.3024211

[8] R. W. Kotla and S. R. Yarlagadda, "Mathematical modelling of SPV array by considering the parasitic effects," *SN Applied Sciences*, vol. 2, no. 50, 2019. doi:10.1007/s42452-019-1861-x

[9] H. D. Tafti, A. I. Maswood, G. Konstantinou, J. Pou, F. Blaabjerg, "A general constant power generation algorithm for photovoltaic systems," IEEE Trans Power Electron, vol. 33, pp. 4088–101, 2018. doi:10.1109/TPEL.2017.2724544

[10] Y. Yang, H. Wang, F. Blaabjerg and T. Kerekes, "A hybrid power control concept for PV inverters with reduced thermal loading," in IEEE Transactions on Power Electronics, vol. 29, no. 12, pp. 6271-6275, Dec. 2014. doi:10.1109/TPEL.2014.2332754

[11] Y. Yang, F. Blaabjerg, H. Wang, "Constant power generation of photovoltaic systems considering the distributed grid capacity," IEEE Appl. Power Electron. Conf. Expo. - APEC 2014, IEEE, pp. 379–85, 2014. doi:10.1109/APEC.2014.6803336

[12] H. D. Tafti, A. Sangwongwanich, Y. Yang, J. Pou, G. Konstantinou and F. Blaabjerg, "An Adaptive Control Scheme for Flexible Power Point Tracking in Photovoltaic Systems," in IEEE Transactions on Power Electronics, vol. 34, no. 6, pp. 5451-5463, June 2019. doi:10.1109/TPEL.2018.2869172

[13] C. Rosa, D. Vinikov, E. Romero-Cadaval, V. Pires and J. Martins, "Low-power home PV systems with MPPT and PC control modes," 2013 International Conference-Workshop Compatibility And Power Electronics, 2013, pp. 58-62. doi:10.1109/CPE.2013.6601129

[14] A. Hoke and D. Maksimović, "Active power control of photovoltaic power systems," 2013 1st IEEE Conference on Technologies for Sustainability (SusTech), 2013, pp. 70-77. doi:10.1109/SusTech.2013.6617300

[15] R. G. Wandhare and V. Agarwal, "Precise active and reactive power control of the PV-DGS integrated with weak grid to increase PV penetration," 2014 IEEE 40th Photovoltaic Specialist Conference (PVSC), 2014, pp. 3150-3155. doi:10.1109/PVSC.2014.6925604

[16] R. W. Kotla, S. R. Yarlagadda, "Grid tied solar photovoltaic power plants with constant power injection maximum power point tracking algorithm," Journal Europeen des Systemes Automatises, vol. 53 issue. 4, pp. 567-573, 2020. doi:10.18280/jesa.530416

[17] H. D. Tafti et al., "Comparative analysis of flexible power point tracking algorithms in photovoltaic systems," 2020 IEEE Energy Conversion Congress and Exposition (ECCE), 2020, pp. 110-115. doi:10.1109/ECCE44975.2020.9236032

[18] A. Urtasun, P. Sanchis and L. Marroyo, "Limiting the power generated by a photovoltaic system," 10th International Multi-Conferences on Systems, Signals & Devices 2013 (SSD13), 2013, pp. 1-6. doi:10.1109/SSD.2013.6564069

[19] S. B. Kjaer, J. K. Pedersen and F. Blaabjerg, "A review of single-phase grid-connected inverters for photovoltaic modules," in IEEE Transactions on Industry Applications, vol. 41, no. 5, pp. 1292-1306, Sept.-Oct. 2005. doi:10.1109/TIA.2005.853371

[20] R. W. Kotla and S. R. Yarlagadda, "Modelling and control of a three phase PVGT system," 2020 IEEE India Council International Subsections Conference (INDISCON), 2020, pp. 96-101. doi:10.1109/INDISCON50162.2020.00031

[21] A. Sangwongwanich, Y. Yang, F. Blaabjerg and D. Sera, "Delta power control strategy for multistring grid-connected PV inverters,"

[22] H. Dehghani Tafti, A. Sangwongwanich, Y. Yang, G. Konstantinou, J. Pou and F. Blaabjerg, "A general algorithm for flexible active power control of photovoltaic systems," 2018 IEEE Applied Power Electronics Conference and Exposition (APEC), 2018, pp. 1115-1121. doi:10.1109/APEC.2018.8341156

[23] A. Sangwongwanich, Y. Yang and F. Blaabjerg, "High-performance constant power generation in grid-connected PV systems," in IEEE Transactions on Power Electronics, vol. 31, no. 3, pp. 1822-1825, March 2016. doi:10.1109/TPEL.2015.2465151

[24] R. W. Erickson, D. Maksimovic, "Fundamentals of power electronics," Norwell, MA, USA: Kluwer, 2001

[25] J. D. Van Wyk, "Power electronics quo vadis?," 2012 15th International Power Electronics and Motion Control Conference (EPE/PEMC), 2012, pp. Session 1-1-Session 1-9. doi:10.1109/EPEPEMC.2012.6397377

[26] A. Zakharov and G. Zinoviev, "Modernization of the test at the course of the "Fundamentals of Power Electronics"," 2014 12th International Conference on Actual Problems of Electronics Instrument Engineering (APEIE), 2014, pp. 815-817. doi:10.1109/APEIE.2014.7040801

NOMENCLATURE

EAPC	Enhanced Active power control
APC	Active power control
MPPT	Maximum power point tracking
PVGT	Photovoltaic Grid Tied
INC	Incremental conductance
V_{mpp}	Maximum power point voltage
P&O	Perturb and observe
P_{pv-out}	Output power from PV
P_{set}	Set power
V_{oc}	Open circuit voltage
P_{pvs}	Power generated from PV string
$P_{INC-mppt}$	Incremental conductance MPPT power output
x	Operating point left of MPP
y	Operating point right of MPP
V_x	Voltage at operating point 'x'
V_y	Voltage at Operating point 'y'
STC	Standard Test Conditions
V_{sc}	Short circuit voltage
ΔV	Instantaneous voltage
$V_{present}$	Voltage at present iteration
$V_{previous}$	Voltage from previous iteration
ΔP	Instantaneous power
$P_{present}$	Power at present iteration
$P_{previous}$	Power from previous iteration
V_{APC}	Voltage at APC mode
T_{APC}	Time period at APC mode
ΔP_{hold}	Threshold power
ΔI	Instantaneous current
D	Duty cycle
G	Irradiance
V_{dc}	DC bus voltage
V_g	Grid voltage
P_{system}	Total PVGT system voltage
$T_{ex-APC-normal}$	Execution Time of APC at healthy conditions
$V_{ex-APC-normal}$	Execution Voltage of APC at healthy conditions
$T_{ex-APC-fault}$	Execution Time of APC at fault conditions
$V_{ex-APC-fault}$	Execution Voltage of APC at fault conditions
$V_{ex-previous}$	Previous executed voltage
$T_{ex-mppt}$	Execution time of INC mppt.
$V_{ex-APC-normal}$	Execution Voltage of INC mppt.
P_{mpp}	Power at MPP
I_{mpp}	Current at MPP
PI	Proportional Integral controller